

JAERI-M
83-190

SECOND HARMONIC ICRF HEATING IN
THE JFT-2M

November 1983

K. ODAJIMA, H. MATSUMOTO, H. KIMURA
T. YAMAMOTO, K. HOSHINO, S. KASAI
T. KAWAKAMI, H. KAWASHIMA, M. MAENO
T. MATOBA, T. MATSUDA, Y. MIURA, M. MORI
H. OGAWA, T. OGAWA, K. OHTA,^{*1} H. OHTSUKA
S. SENGOKU, T. SHOJI, N. SUZUKI, H. TAMAI^{*2}
Y. UESUGI, S. YAMAMOTO, T. YAMAUCHI
I. YANAGISAWA,^{*3} H. NAKAMURA and
M. KATAGIRI

JAERI-M レポートは、日本原子力研究所が不定期に公刊している研究報告書です。
入手の問合わせは、日本原子力研究所技術情報部情報資料課（〒319-11 茨城県那珂郡東海村）
あて、お申しこしてください。なお、このほかに財団法人原子力弘済会資料センター（〒319-11 茨城
県那珂郡東海村日本原子力研究所内）で複写による実費頒布をおこなっております。

JAERI-M reports are issued irregularly.
Inquiries about availability of the reports should be addressed to Information Section, Division
of Technical Information, Japan Atomic Energy Research Institute, Tokai-mura, Naka-gun,
Ibaraki-ken 319-11, Japan.

© Japan Atomic Energy Research Institute, 1983

編集兼発行 日本原子力研究所
印刷 山田軽印刷所

Second Harmonic ICRF Heating in the JFT-2M

Kazuo ODAJIMA, Hiroshi MATSUMOTO, Haruyuki KIMURA
Takumi YAMAMOTO, Katsumichi HOSHINO, Satoshi KASAI
Tomohide KAWAKAMI, Hisato KAWASHIMA, Masaki MAENO
Toru MATOBA, Toshiaki MATSUDA, Yukitoshi MIURA
Masahiro MORI, Hiroaki OGAWA, Toshihide OGAWA
Kanji OHTA^{*1}, Hideo OHTSUKA, Seio SENGOKU
Teruaki SHOJI, Norio SUZUKI, Hiroshi TAMAI^{*2}
Yoshihiko UESUGI, Shin YAMAMOTO, Toshihiko YAMAUCHI
Ichiro YANAGISAWA^{*3}, Hiroo NAKAMURA⁺¹ and Masaki KATAGIRI⁺²

Department of Thermonuclear Fusion Research,
Tokai Research Establishment, JAERI
(Received October 20, 1983)

Pure second harmonic ion cyclotron heating experiments in hydrogen plasma were carried out in the JFT-2M tokamak. In order to improve an absorption characteristics in the second harmonic regime, neutral beam injection heating is used, and effective heating via ICRF is observed. With 550kW of NBI, the plasma is heated up to $T_i=0.9\text{keV}$, and $T_e=1.1\text{keV}$. 30ms after the start of NBI, 520kW of ICRF is applied and plasma is finally heated up to $T_i=1.1\text{keV}$, $T_e=1.6\text{keV}$. Magnetic measurement of $\Lambda+1/2 = \beta_p + (\ell_i - 1)/2$ increases by $\Delta\Lambda=0.3$ with ICRF heating.

Preliminary coupling study of a wave guide coupler is also investigated. A parallel plate TEM electric field coupler, whose electric field configuration is almost the same as a ridged wave guide, are used

+1 Department of Large Tokamak Development, Tokai, JAERI

+2 Department of Reactor Engineering, Tokai, JAERI

*1 On leave from Mitsubishi Electric Co.

*2 On leave from Tsukuba University

*3 On leave from Mitsubishi Atomic Power Industries, Inc.

as a simulator of a ridged wave guide coupler. The transmission coefficient with plasma is almost the same as the one obtained by loop antenna at low power level.

Keywords; ICRF Heating, JFT-2M Tokamak, Plasma Heating, Hydrogen Plasma Wave Guide Coupler, Neutral Beam Injection, Temperature, Second Harmonic Regime

JFT-2Mにおける2倍高調波ICRF加熱

日本原子力研究所東海研究所核融合研究部

小田島和男・松本 宏・木村 晴行・山本 巧
星野 克道・河西 敏・河上 知秀・川島 寿人
前野 勝樹・的場 徹・松田 俊明・三浦 幸俊
森 雅博・小川 宏明・小川 俊英・大田 完治^{*1}
大塚 英男・仙石 盛夫・荘司 昭朗・鈴木 紀男
玉井 広史^{*2}・上杉 喜彦・山本 新・山内 俊彦
柳沢 一郎^{*3}・中村 博雄⁺¹・片桐 政樹⁺²

(1983年10月20日受理)

水素プラズマ中における純2倍高調波イオンサイクロトロン周波数における加熱実験がJFT-2Mで行われた。2倍高調波領域における吸収を改善するために中性粒子入射加熱を用い、有効な加熱結果を観測した。550 kWのNBIによりプラズマは $T_i = 0.9$ keV, $T_e = 1.1$ keVまで加熱され、ICRF 520 kWにより、 $T_i = 1.1$ keV, $T_e = 1.6$ keVまで温度が上昇した。 $A + \frac{1}{2}$ の磁気測定でICRFによる上昇分 $\Delta A = 0.3$ を得た。

導波管結合の予備実験を開始した。リッジ導波管結合器のシミュレータとして、電界配位がほぼ等しい、平行2板電界結合器を製作し、1 Wレベルでの結合度を測定した。その結果ループアンテナとほぼ同じ値が得られた。

+1 大型トカマク開発部

+2 原子炉工学部

*1 外来研究員；三菱電機(株)

*2 特別研究生(筑波大学)

*3 外来研究員；三菱原子力工業(株)

Contents

| | |
|------------------------------------------------------------|----|
| 1. Introduction | 1 |
| 2. Apparatus | 3 |
| 3. Experiment | 5 |
| 4. Coupling Experiment of TEM Electric Field Coupler | 8 |
| 5. Discussion and Conclusions | 10 |
| Acknowledgement | 12 |
| References | 13 |

目 次

| | |
|-------------------------|----|
| 1. 序 文 | 1 |
| 2. 装 置 | 3 |
| 3. 実 験 | 5 |
| 4. TEM電界結合器での結合実験 | 8 |
| 5. 議論と結論 | 10 |
| 謝 辞 | 12 |
| 参考文献 | 13 |

1. Introduction

Recently main objectives of tokamak experiments have moved to additional heatings and the plasma properties associated with them. Ion cyclotron range of frequency (ICRF) heating is one of the most promising schemes among various additional heating methods. In the last few years, much progress has been made^{1~3)} both in physics and technical aspect of ICRF heating.

In a tokamak plasma, it is known that the minority hydrogen in a deuterium plasma produces two-ion hybrid resonance layer at the higher magnetic field side of the fundamental cyclotron resonance layer of minority protons. The impressed ICRF field generates a fast magnetosonic wave beyond the evanescent region in the peripheral plasma. This wave propagates to the hybrid resonance layer and is converted to an ion Bernstein wave near the layer. The energy of the wave which is converted to the ion Bernstein wave is efficiently transferred to the three species of particles, deuterons, protons, and electrons.⁴⁾

In second harmonic heating case, in which minority component plasma is absent, a mode coupling layer also exists close to the second harmonic cyclotron resonance layer in the high field side as in the two-ion hybrid scheme. The thickness of this layer is proportional to $\beta_i R_0$, where β_i is the local ion toroidal betavalue and R_0 is the major radius. In this layer, mode coupling to ion Bernstein waves and enhanced harmonic cyclotron damping can occur. We can thus expect the plasma heating in the second harmonic regime.⁵⁾

The second harmonic scheme has favorable characteristics to heat a reactor plasma; it does not need a minority component, and a high energy ion tail produced by the heating can enhance a nuclear fusion reactivity. In present tokamaks, this scheme allows us to use hydrogen plasma which is free from neutron radiation. This is quite convenient in a high β regime experiments, since we do not have to shield the machine against the neutron damages.

With the given magnitude of magnetic field, the frequency is two times as high as that of the two ion scheme. This high frequency enables us to use wave guide launcher instead of loop antenna as a coupling structure.

In order to apply the ICRF heating to a reactor, the simple structure of the wave guide is more favorable than the loop antenna. Then we must test the wave guide coupling to prove its effectiveness by comparing with the loop antenna coupling.

The heating experiment in the second harmonic regime is tried in the PLT.²⁾ In this experiment, the high energy tail is observed in a perpendicular charge exchange ion spectrum. The increment of average ion energy is almost the same as that of minority hydrogen scheme. But the increase of electron temperature or poloidal beta value is still not clear.

In this paper, the heating results in the second harmonic regime are investigated in the NBI heated plasma. It is shown that both electron and ion temperatures increase and this increment is consistent with the magnetic measurement of poloidal beta value.

In section 2, experimental configurations are mentioned. Results of heating experiment are shown in section 3. In section 4, we show a coupling results from a TEM electric field couler, which simulate the ridged wave guide. In the last section, conclusions and discussion are presented.

2. Apparatus

JFT-2M is a tokamak with D shaped vacuum vessel with 1.31m major radius and 0.415 x 0.595m minor radius. In the present experiment, the machine is operated with circular cross section and the plasma radius is limited by inner and outer limiter at $a=35$ cm. The limiter material is carbon graphite.

The rf generator is operated at 38 MHz which is the second harmonic cyclotron frequency of protons with the toroidal magnetic field $B_T=12.5$ kG. The output power of generator which has single TH116 power triode is about 0.8 MW at the 50Ω dummy load, and the maximum pulse duration is 50ms.

Fig.1 shows a top view of JFT-2M and the arrangement of diagnostic instruments. Electron temperature is measured with soft X-ray pulse height analyzer. Energy spectra of hydrogen and deuterium ions are measured with E//B mass sensitive charge exchange neutral analyzer at the same time.⁷⁾ The measurement is carried out in slightly off perpendicular direction (14°) with respect to the toroidal magnetic field. The energy spectrum measured in this direction is not affected by ripple-trapped particles.

The increase of poloidal beta value β_p is measured by B_θ probes at inner and outer side of the torus, and by saddle loops (half turn closed flux loops).⁸⁾ The value $\Lambda + 1/2 = \beta_p + \ell_i / 2 - 1/2$, where ℓ_i is internal inductance which is related to the plasma current profile, is obtained from this measurement. There are two possibilities in the increase of $(\Lambda + 1/2)$. Those are the increase of β_p , and the increase of ℓ_i due to an edge cooling by impurity radiation. But 1-D tokamak simulation code including internal disruption indicates that the change in ℓ_i value is very small, typically within 0.06 in the case of safety factor at limiter radius $q_a=3$, because the q value at the center of the plasma is almost fixed around 1 by the internal disruption. Thus, when the change of $(\Lambda + 1/2)$ is sufficiently large, typically larger than 0.1, $\Delta\Lambda$ is attributed to the change of β_p .

The antenna is shown in Fig.1. This is a quarter turn loop located at the

outer side (lower magnetic field side) of the torus. The radiative region of the antenna is 50cm in length and 7 cm in width. The coupling resistance is critically dependent on the horizontal plasma position. Figure 2 shows the coupling resistance versus horizontal plasma position. The solid line is a calculated value by three dimensional model. The resistance decreases by a factor of 5 with inward plasma shift of 7cm. In the optimum condition, the coupling efficiency is about 85%. The main loss is attributed to an ohmic dissipation in the region between the vacuum feedthrough and the radiative part of the loop which is bent to the toroidal direction so as to avoid an interference with a horizontal port section. The Faraday shield is optimized so as to minimize an ohmic loss at the screen.⁶⁾ The loss is estimated to be 0.084Ω by the calculation and is negligible compared to the vacuum loading resistance, 0.32Ω .

3. Experiment

Typical experimental conditions are as follows; plasma current $I_p = 170 \sim 180$ KA, the strength of toroidal magnetic field $B_T = 12.5$ KG, in which second harmonic ion cyclotron layer is at the center of plasma, and line average electron density $\bar{n}_e = 2.5 \sim 3 \times 10^{13} \text{ cm}^{-3}$ during the heating.

When more than 100KW of RF is applied to the joule heated plasma, a disruption occurs mainly because of the large increase of radiation loss. The charge exchange spectra before and after the rf is switched on are shown in Fig.4. The significant high energy tail is observed and bulk ion temperature which is determined by the inclination between 1.5keV and 4.5keV increases about 50eV. An appreciable increase of electron temperature is not observed. The magnetic measurement of $(\Lambda + 1/2)$ increases slightly as shown in Fig.5(a). The increment is 0.03 and we cannot conclude the increase of plasma pressure. These results seem to be due to weak absorption of the rf power, because of low β_i value at the plasma center.

In the case of second harmonic heating, the following merits are expected in the NBI heated plasma; (i) higher temperature and higher β plasma absorb the rf power more effectively, (ii) high energy ion component produced by NBI enhances the absorption of rf power.⁹⁾ (iii) neutral beam stabilizes the disruption by compensation the radiation loss. Thus, 600KW of rf power has been coupled to the plasma with assist of NBI.

Figure 5(b) shows $(\Lambda + 1/2)$ during the rf heating in 240KW of NBI heated plasma. The rf net power is almost the same as Fig.5(a), and the increment is about 0.1. This value is sufficiently meaningful value compared to the variation of $\beta_i/2$. It should be noted that in the NBI heated plasma, the second harmonic heating is more effective than in the joule plasma.

Time evolution of plasma parameters before and during the NBI and ICRF heating are shown in Fig.6. RF power is applied 30ms after the initiation of NB co-injection. With 550KW of NBI, the plasma is heated up to $T_i = 0.9$ keV

and $T_e = 1.1\text{keV}$. Then 520kW of ICRF power heats plasma up to $T_i = 1.1\text{keV}$ and $T_e = 1.6\text{keV}$. The increment of plasma pressure Δn from joule phase to NBI heated phase is about 0.2 and from NBI heated phase to ICRF heated phase is about 0.3. These values obtained with magnetic measurement are consistent with the temperature measurement on the assumption that the electron temperature profile is peaked by the ICRF heating. This assumption is reasonable because the increased radiation loss cools the peripheral region of the plasma. The increment of the radiation loss becomes almost the same as the ICRF input power.

Figure 7(a) shows the increase of plasma pressure Δn as the function of hydrogen concentration ratio of hydrogen-deuterium two ion plasma with the injection of hydrogen neutral beam. Δn increases with the increase of hydrogen component. Considering that deuterium does not contribute to the wave damping because the deuterium has only the fourth harmonic cyclotron resonance, this shows that the heating efficiency is determined by the wave damping at the hot core of the plasma. The radiation loss and carbon impurity increase with the decrease of Δn as shown in Fig.7(b).

The increase of other impurities during the ICRF heating is shown in Fig.8. Figure 8(a) is the case of hydrogen plasma with hydrogen NBI. Fig 8(b) is the case of deuterium plasma with hydrogen NBI. The latter case is rather weak heating as can be seen in Fig.7. It should be noted that in both cases, the increment of metallic impurities such as titanium and iron, and oxygen impurities due to ICRF heating are almost the same. But the increment of carbon impurity is clearly different. The carbon impurity in the hydrogen case hardly increases. On the contrary, that in the deuterium case increases significantly.

The carbon is only used at the limiter, and the titanium is only used at Faraday shield of the antenna in the JFT-2M vacuum vessel. Close to the loop antenna, there is TEM electric field coupler, whose side is made of stainless steel. This has a possibility as an iron source, and other parts of the inner vacuum vessel are made of stainless steel. Thus location of metallic impurity

sources in the vacuum vessel can be distinguished.

From the evolution of impurities shown in Fig.8, we can think about two kinds of impurity production mechanisms. One is the mechanism with no correlation to the absorption of the launched wave in the plasma. Metallic impurities from the antenna are released by this mechanism. The other is the one which has some correlation to the absorption of the wave. Carbons are released by this mechanism.

The former mechanism would be considered as follows. Certain percentage of the rf power radiated from the antenna is directly deposited near the antenna and the materials of the antenna are sputtered out. This mechanism may be simple acceleration of the rf electric field because the source of impurity is restricted around the antenna.

The possible explanation of the latter mechanism would be as follows. When the rf power absorption in the hot core is weak, the rf power can be absorbed in a peripheral region resulting in the release of carbon impurity. This mechanism has strong correlation with the strength of the rf power absorption in the hot core region.

In the present experiment, oxygen impurity is dominant. Rough estimation of impurity concentration indicates that the dominant impurity which contributes to radiation loss is oxygen.⁸⁾ Thus the metallic impurities are not so harmful compared to the oxygen impurities in the present JFT-2M experiments. But the thorough discharge clearing and/or titanium gettering decrease the oxygen, and in the future experiment with high power ICRF, the metallic impurities will play a dominant role in power balance at the center and have a harmful effect on the plasma confinement. In order to reduce the metallic impurities during the ICRF heating, it is necessary to reduce the impurities released from the antenna region.

4. Coupling experiment of TEM electric field coupler

In order to simulate a ridge wave coupling, TEM electric field coupler is used.¹⁰⁾ Figure 9 shows the coupler. It consists of two parallel plates in a shield box. The parallel plate is 30cm in width and 2cm in thickness. The shield box has rectangular cross section with 40 x 48cm. The gap distance between the two parallel plates can be changed from 0 to 10cm. This enables us to study the optimization of the electric field coupling. The mouth of the coupler is 6cm in length and is opened by 60° in order to improve the coupling with the plasma.¹¹⁾

The rf power is fed from upper and lower sides with opposite phase. Thus the two parallel plates act as parallel transmission lines. The electric field in the gap is vertical to the parallel plates. Configuration of electric field lines in this parallel plates is almost the same as that of the ridge wave guide.

When the gap distance is sufficiently small compared to the dimension of the shield box, almost all of the rf energy is concentrated in the gap. There is an electric field parallel to the magnetic field line around the edge of the parallel plates. The gap width of the parallel plates is selected so as to minimize the electric field directed to the magnetic field.

In order to shield the electric field in the direction of magnetic field, a simple Faraday shield is placed in front of the mouth of the coupler. This Faraday shield consists of square rods (5mm x 5mm) placed in the direction of magnetic field lines at intervals of 2cm.

The power transmission coefficient is defined by $(1 - \Gamma^2) = 4\rho / (\rho + 1)^2$, where Γ is reflection coefficient and ρ is voltage standing wave ratio in the 50 Ω coaxial line. The voltage standing wave ratio is determined by,

$\rho = (V_f + V_r) / (V_f - V_r) = (V_f + V_r)^2 / (V_f^2 - V_r^2)$, where V_f and V_r are forward and reflection voltage measured by directional coupler, and $(V_f^2 - V_r^2)$ is the transmission power from the generator.

Fig.10 shows the transmission coefficient as a function of a gap distance of the parallel plates. The transmission coefficient increases almost linearly with the gap distance. With the injection of hydrogen neutral beam, the

coefficient becomes three times as large as that without NBI.

Theoretical analysis by three dimensional coupling code predicts that the transmission coefficient is several percents and that it is almost proportional to the gap distance. In the experiment, the transmission coefficient was proportional to the gap distance, but the absolute values were 2 ~ 5 times as large as the theoretical values. Three dimensional full wave code also predicts that the transmission coefficient increases with the increase of the fast wave absorption in the plasma.¹²⁾ This prediction was confirmed in the experiment by changing the absorption in the plasma by neutral beam injection. But transmission coefficients observed in the experiments were almost the same in the hydrogen plasma and in the deuterium plasma.

The coupling measurement of electric field coupler is only preliminary and high power heating experiment is now under way.

5. Discussion and conclusions

Second harmonic ICRF heating was successfully demonstrated in JFT-2M. Since profile measurements were not available in the experiment, 1-D tokamak code simulation was made to estimate the power balance of the heating upon following assumptions. $X_e = 1 \times 10^{19} / n_e$, $X_i = 1.5X_{NC}$ in the joule phase, $X_e = 2 \times 10^{19} / n_e$, $X_i = 1.5X_{NC}$ during the heating. During the rf heating, neutral beam is also injected. This enhancement of electron heat conductivity during NBI was observed in JFT-2 experiment. Also preliminary result of NBI experiment in JFT-2M shows the same tendency.

The rf power deposition on ions with flat profile within $r=10\text{cm}$ and deposition on electrons within $r=15\text{cm}$ were simply assumed. Experimental results are well simulated by the time evolution of total rf power deposition on electrons and ions shown in Fig.11. During the first $10 \sim 20\text{ms}$ of the heating period, the rf deposition to electrons is not significant. In later period, deposition to electrons should be quite significant.

Although profile data are not available and this simulation is only presumable, we can say that more than half of the rf heating power is absorbed by electrons in the second harmonic regime. This result is inconsistent with the theoretical works using 1-D kinetic full wave equation in a bounded plasma.¹³⁾ There are two possible mechanism which can explain the electron heating in this experiment; (1) mode converted ion Bernstein wave heats electrons by Landau damping. (2) High energy beam ions are preferentially heated, and energy which flows from the beam ions to electrons is enhanced.

The former mechanism seems reasonable, and the rf power deposition to electrons seems to increase with the increase of electron temperature. This can be due to the enhancement of Landau damping resulting from the increase of electron temperature. But the theoretical analysis still cannot explain the experimental results by this mode conversion. As for the latter mechanism, high energy ions above 30keV can preferentially transfer energy to electrons. We do not observe enhancement of such high energy part by the present charge exchange analyzer.

Our experiment is very preliminary and further experiments are needed for the complete understanding of second harmonic heating. The experimental results are summarized as follows.

(1) Second harmonic ICRF heating is successfully demonstrated in the JFT-2M. Both electron and ion temperature increase by applying ICRF to the NBI heated target plasma. The increase of plasma energy is confirmed in the magnetic measurements of poloidal beta. On the other hand, with the joule heated target plasma, the heating results are poor in spite of the production of high energy tail in the ion charge exchange spectrum.

(2) Two kinds of impurity production mechanisms are distinguished. The one is not related to the absorption of the wave in hot core, and this mechanism produces impurities from the antenna region. The other is strongly correlated to the absorption of the wave. Limiter materials is released into the plasma by this mechanism.

(3) Preliminary coupling study of wave guide coupler is investigated. A parallel plate TEM electric field coupler, whose electric field configuration is almost the same as that of a ridged wave guide, is used. The transmission coefficient of the wave from the parallel plated launching structure into the plasma is almost the same as the one obtained by loop antenna at low power level.

Acknowledgements

The authors are grateful to the members of the JFT-2 operation groups for their excellent operation and helpful supports. Stimulating discussion with Drs. K.Itoh, A.Fukayama and S.I.Itoh are gratefully acknowledged. Concerning the design of TEM electric field coupler, valuable suggestions are obtained from Prof.Goto of Tokyo Institute of Technology. We also sincerely thanks to him. Drs. Y.Tanaka, M.Tanaka, Y.Obata, Y.Iso and S.Mori are appreciated for their continuous encouragements.

References

1. H. Kimura, et al, Proc. 9th International Conference on Plasma Physics and Controlled Nuclear Fusion Research(Baltimore, 1982) Vol.II, 113 IAEA-CN-41/J-3.
2. D.Q. Hwang, et al., ibid. IAEA-CN-41/I-1.
3. Equipe TFR, ibid. IAEA-CN-41/I-2.
4. S. Iizuka, et al., Phys. Rev. Lett. 45, 1256(1980).
5. D.G. Swanson, Nuclear Fusion 20, 949(1980).
6. D.W. Faulconer, et al., "Adverse shielding of heating field and high ohmic loss introduced by electrostatic shields in RF heating of Plasma." to be published in Jr. of App. Phys. 1983.
7. Y. Miura et al., "Analysis of Charge Exchange Spectra during ICRF Heating in JFT-2 Tokamak." to be published in Nuclear Fusion.
8. T. Shoji, et al., Proc. 11th Europ. Conf. on Controlled Nuclear Fusion and Plasma Physics(Achen, 1983) Vol.I, 55.
9. S.I. Itoh, et al., " Simultaneous heating by ICRF wave and NBI" to be published in Nuclear Fusion.
10. N. Goto, (Tokyo Institute of Technology) , private communication.
11. N. Goto, private communication.
12. K. Itoh, et al., " Three dimensional structure of ICRF waves in Tokamak plasmas". to be published in Nuclear Fusion. & " Excitation of ICRF waves in Tokamaks by wave guide launcher." . HIFT-85(Hiroshima Univ. 1983).
13. A. Fukuyama, et al., Nuclear Fusion 23, 1005(1983).

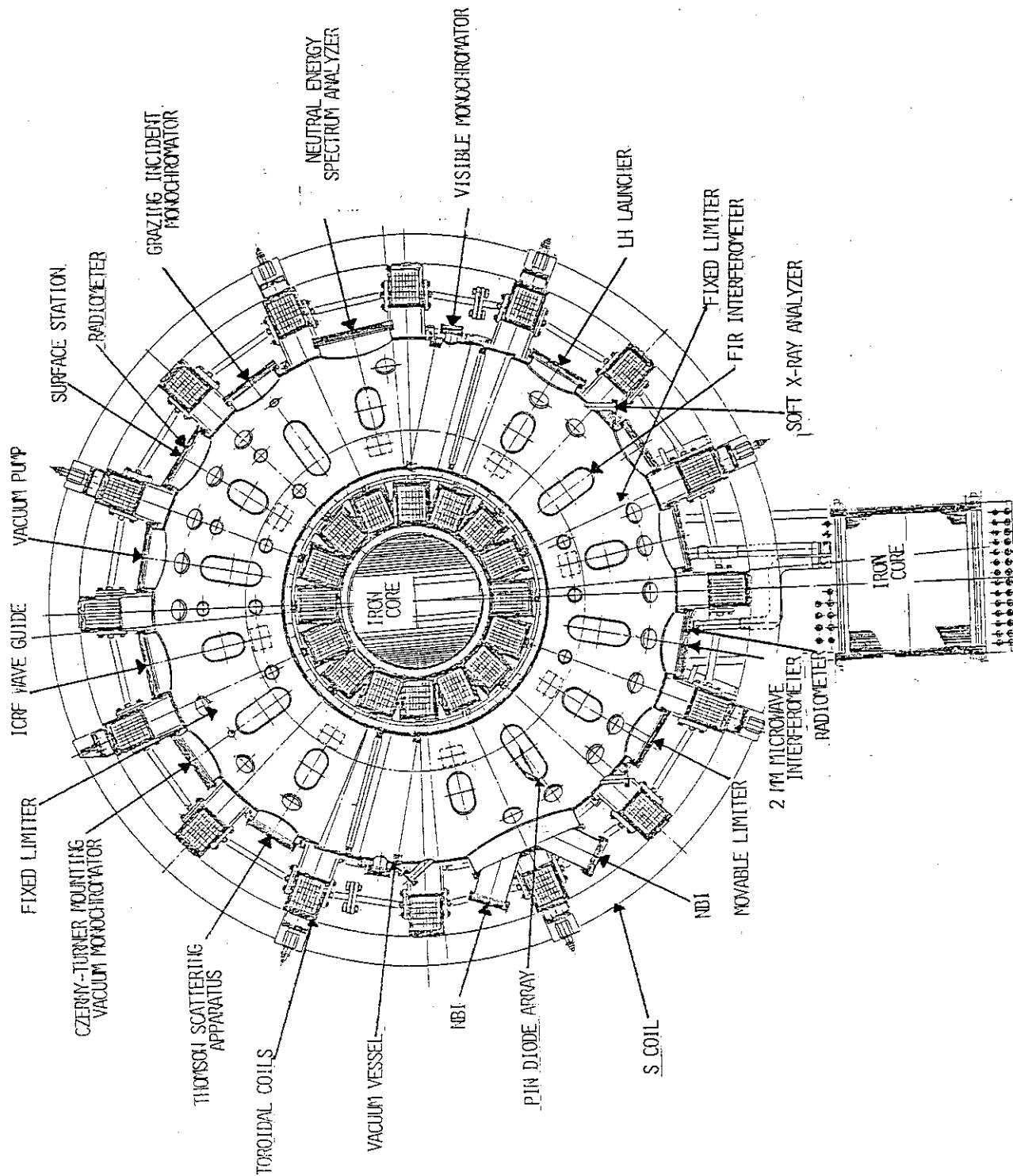


Fig.1 Top view of JFT-2M and the arrangement of diagnostic instruments.

JFT - 2M Loop Antenna
Loading Resistance
vs. Plasma Position

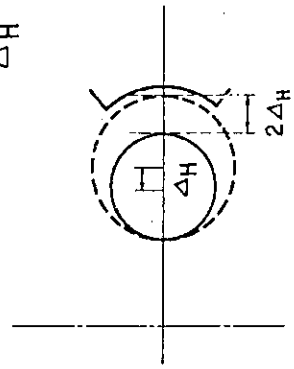
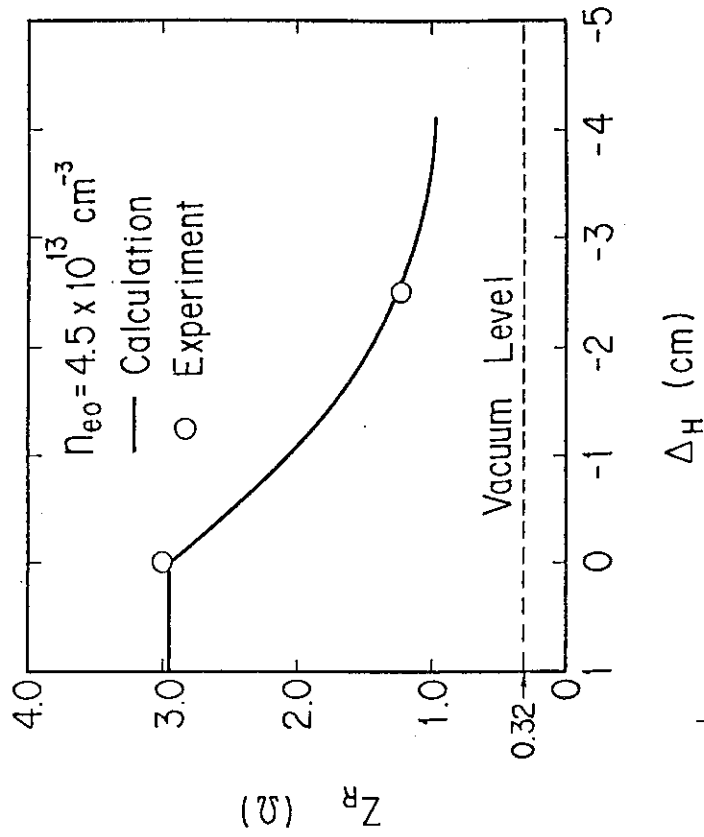


Fig.3 Coupling resistance versus horizontal plasma position

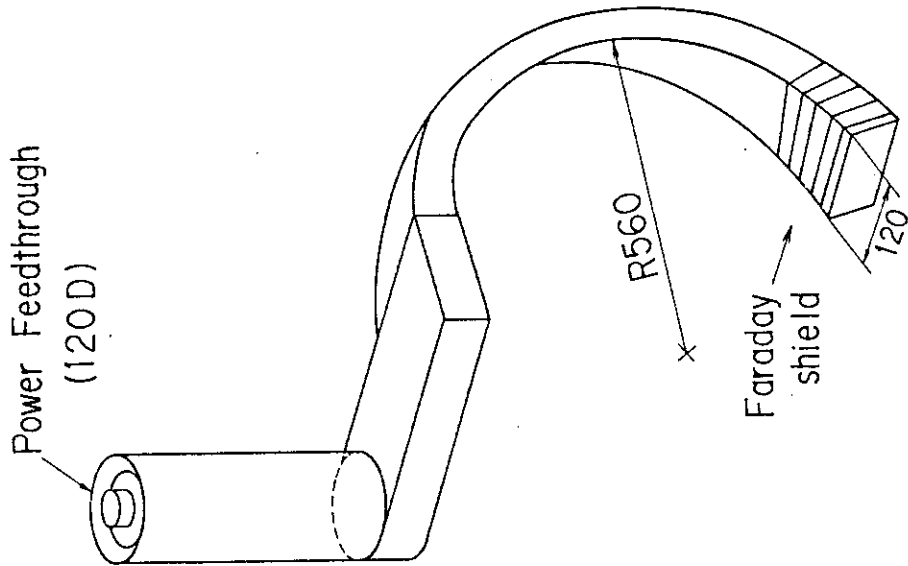


Fig.2 Figure of the JFT-2M loop antenna

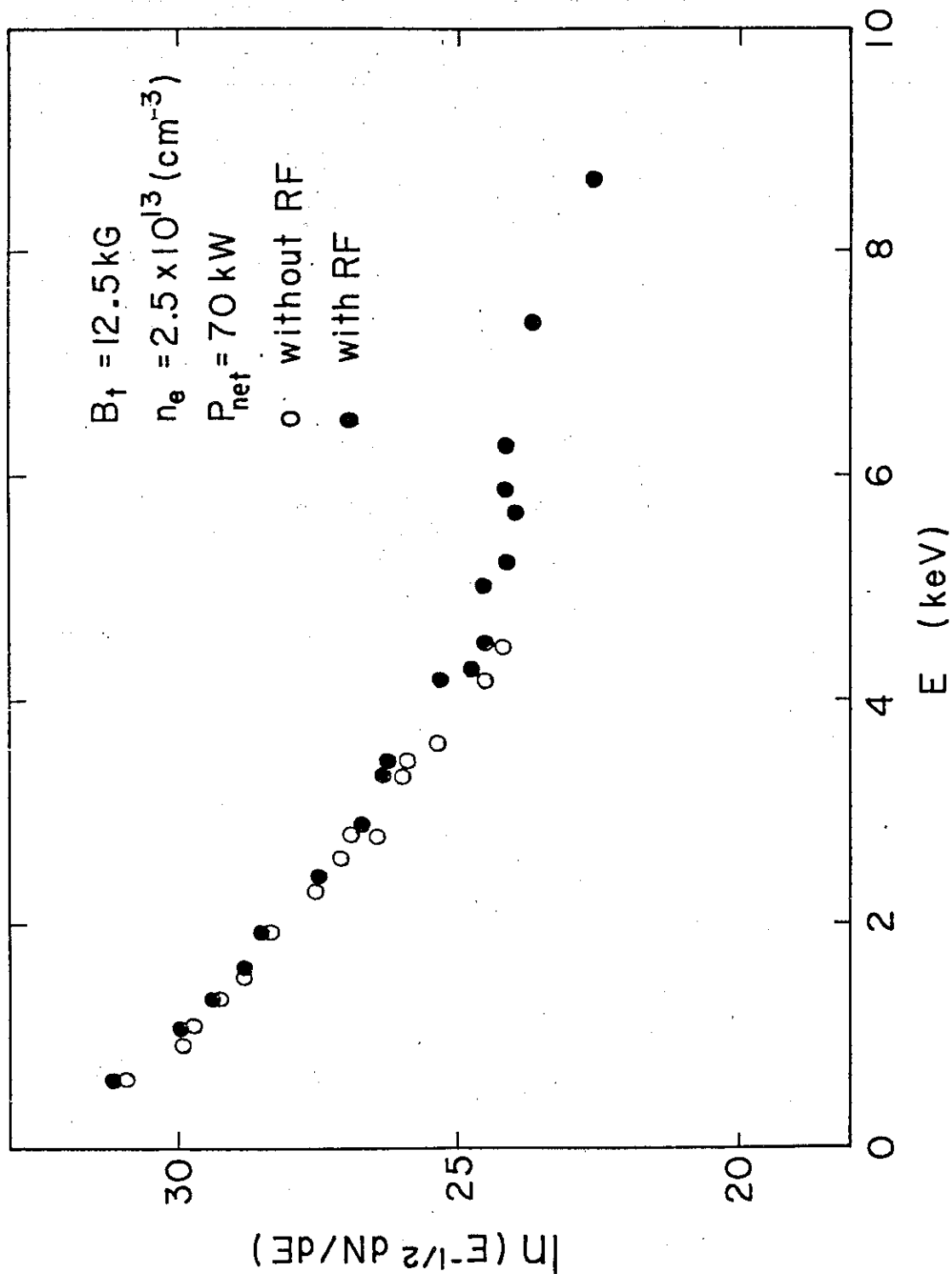


Fig.4 Charge exchange spectrum before and after the onset of the RF heating.

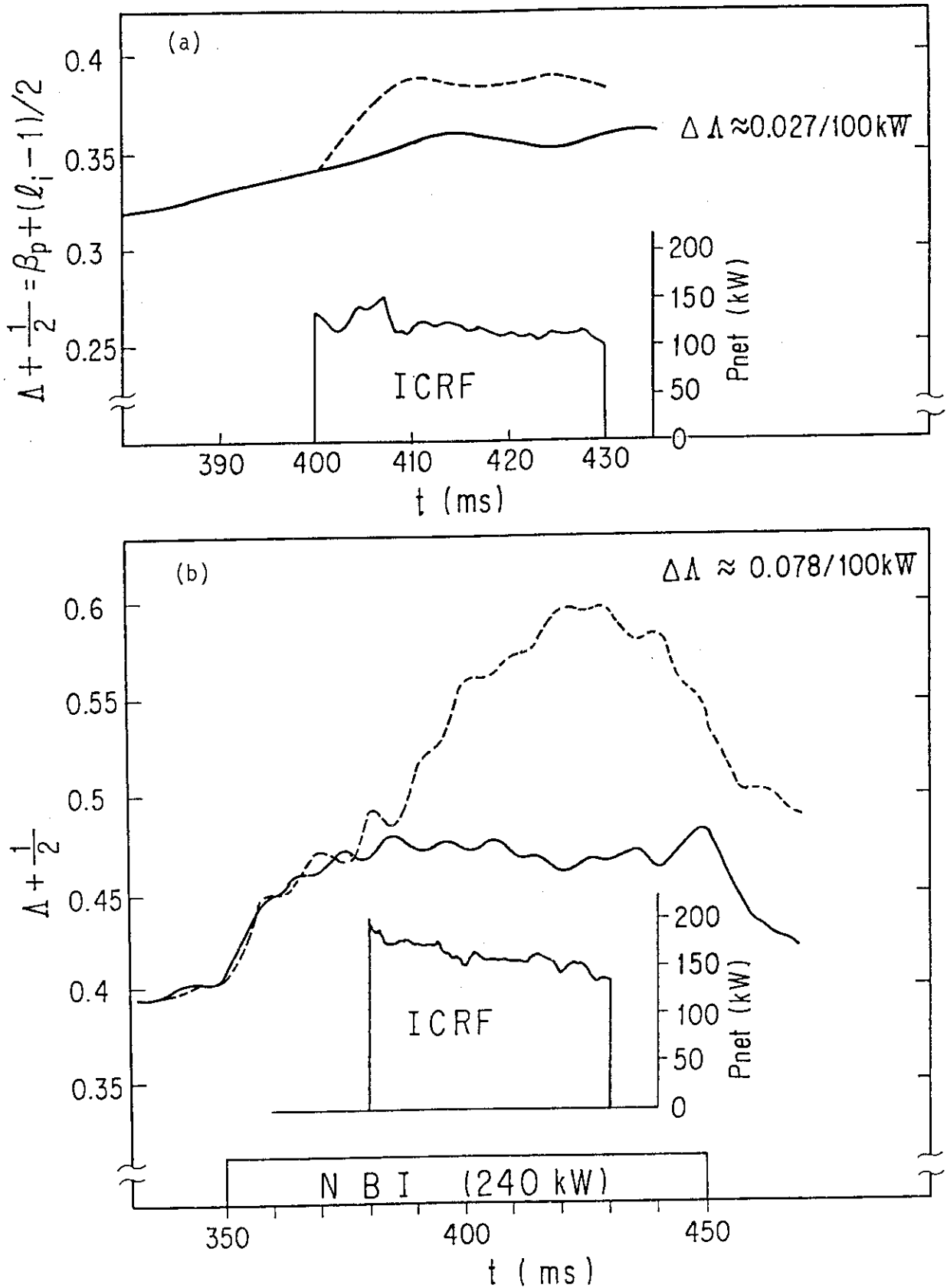


Fig.5 Increase of $\Delta + 1/2$ by the second harmonic ICRF heating (a) without NBI (b) with NBI

Hydrogen Plasma

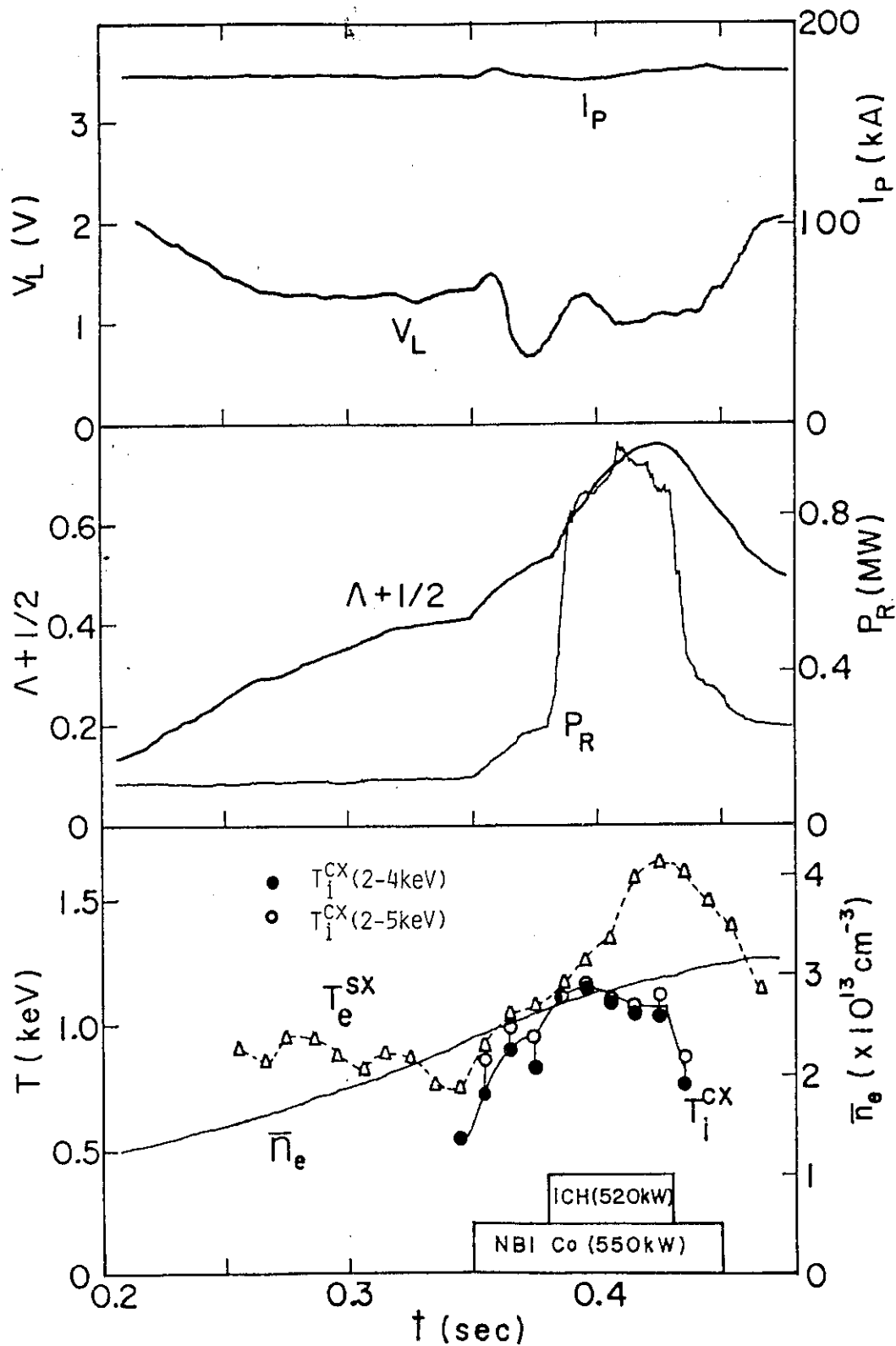


Fig.6 Time evolution of plasma parameters in the second harmonic ICRF heating with NBI.

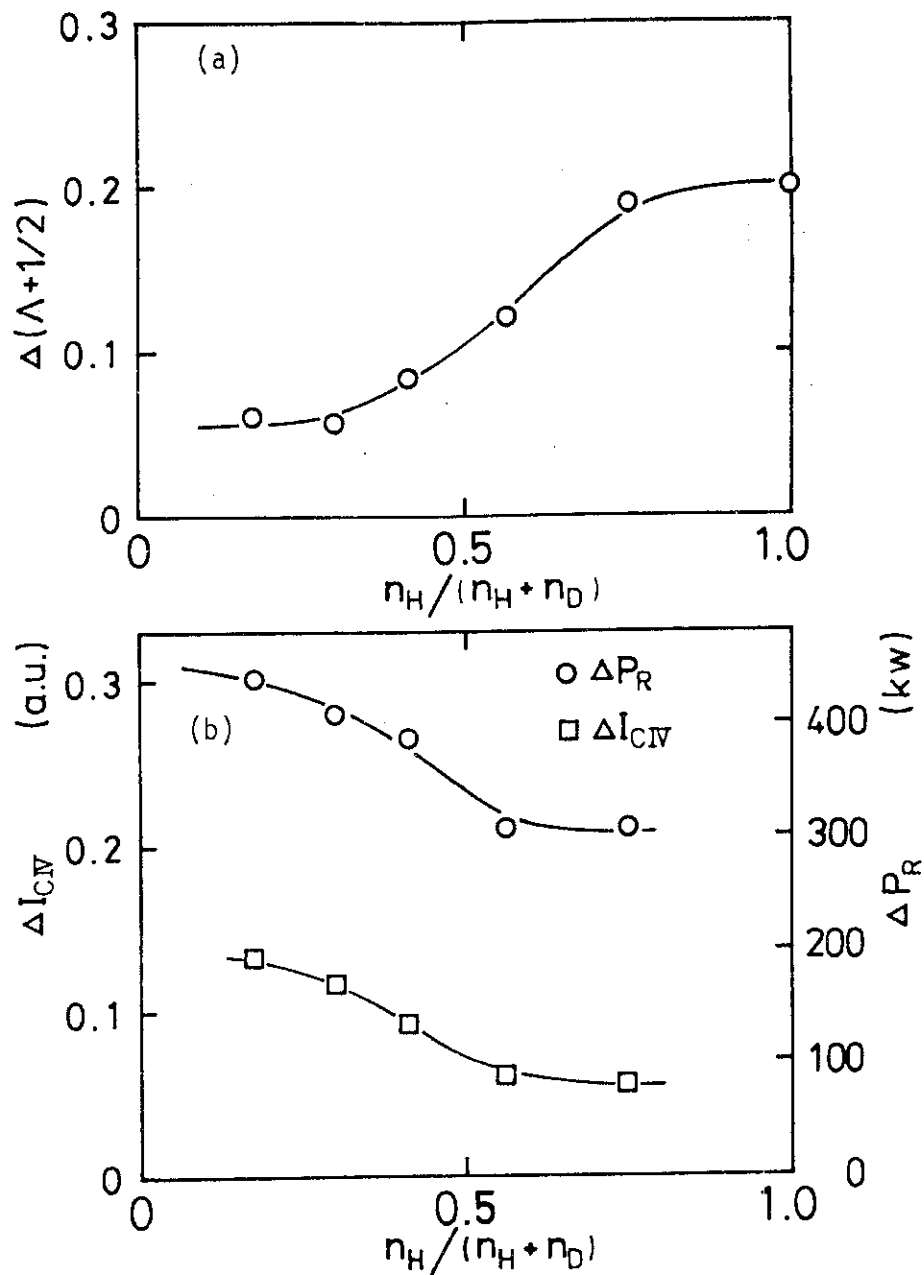


Fig.7 (a) Increase of plasma pressure $\Delta\Lambda$ as a function of hydrogen concentration ratio in hydrogen-deuterium two ion plasma. (b) Increments of radiation loss and carbon impurity by ICRF heating as a function of the hydrogen concentration ratio.

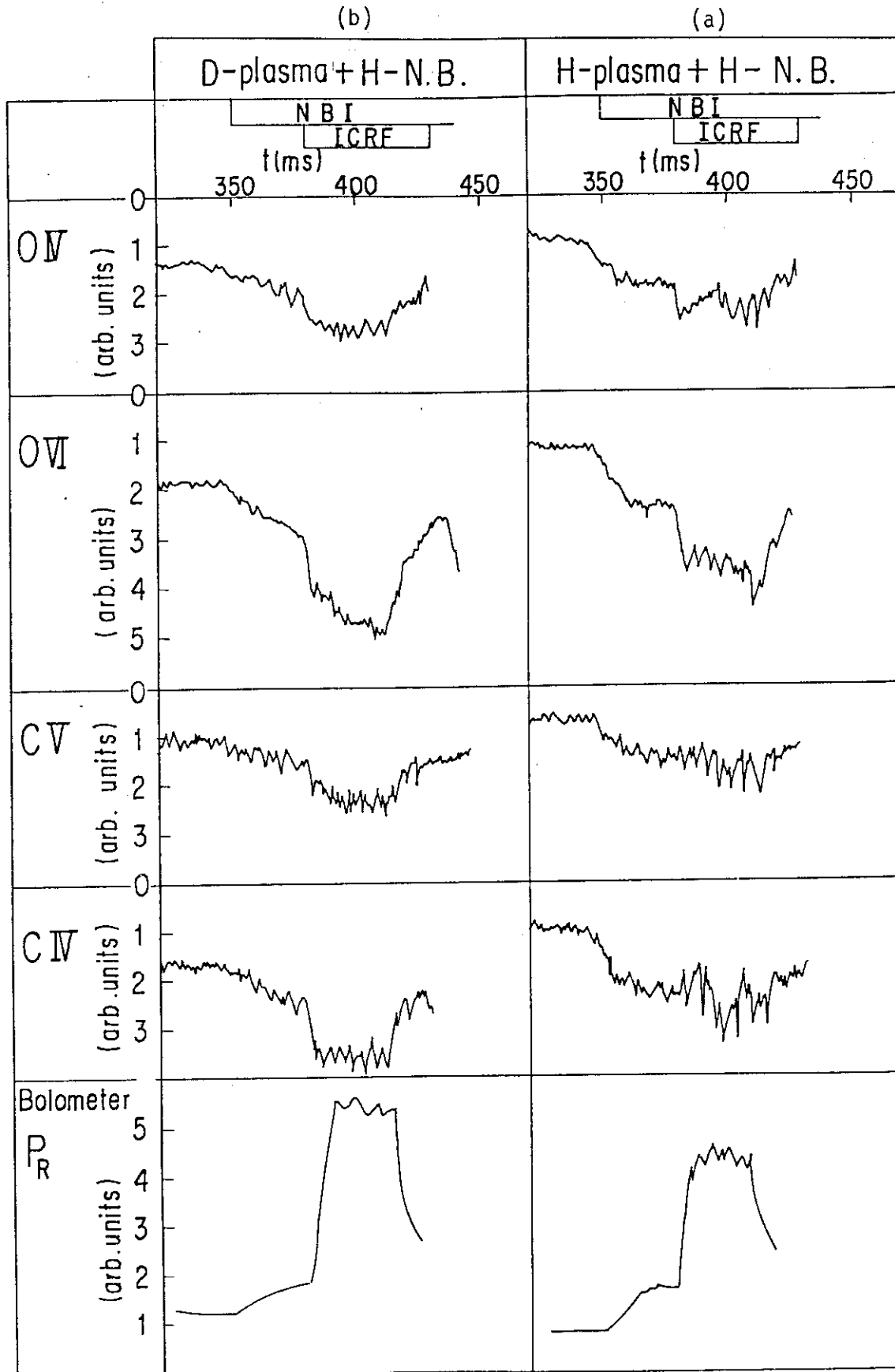


Fig.8 Time evolution of impurity line intensity during the heating (a) with hydrogen plasma (b) with deuterium plasma.

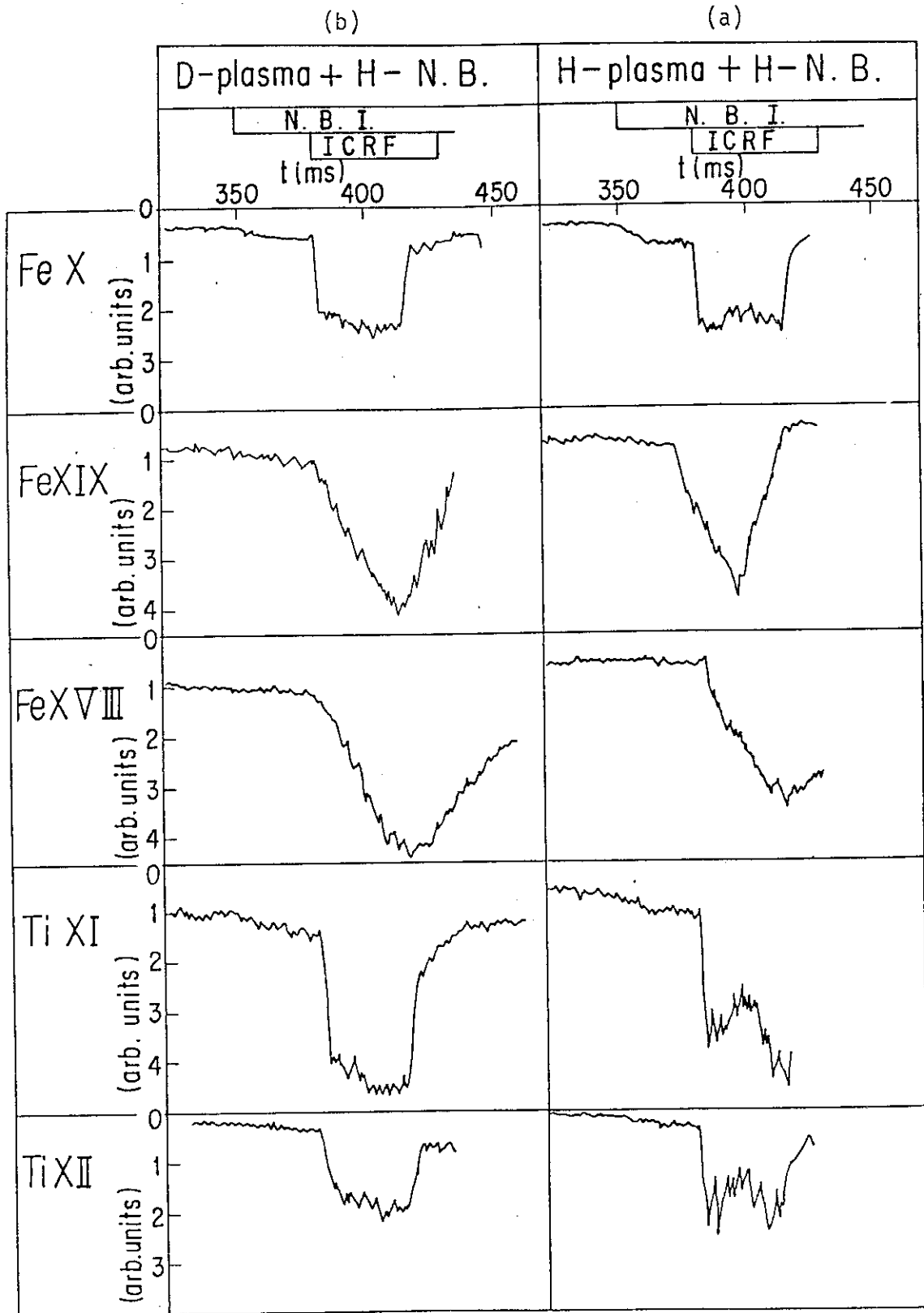


Fig.8 Continued

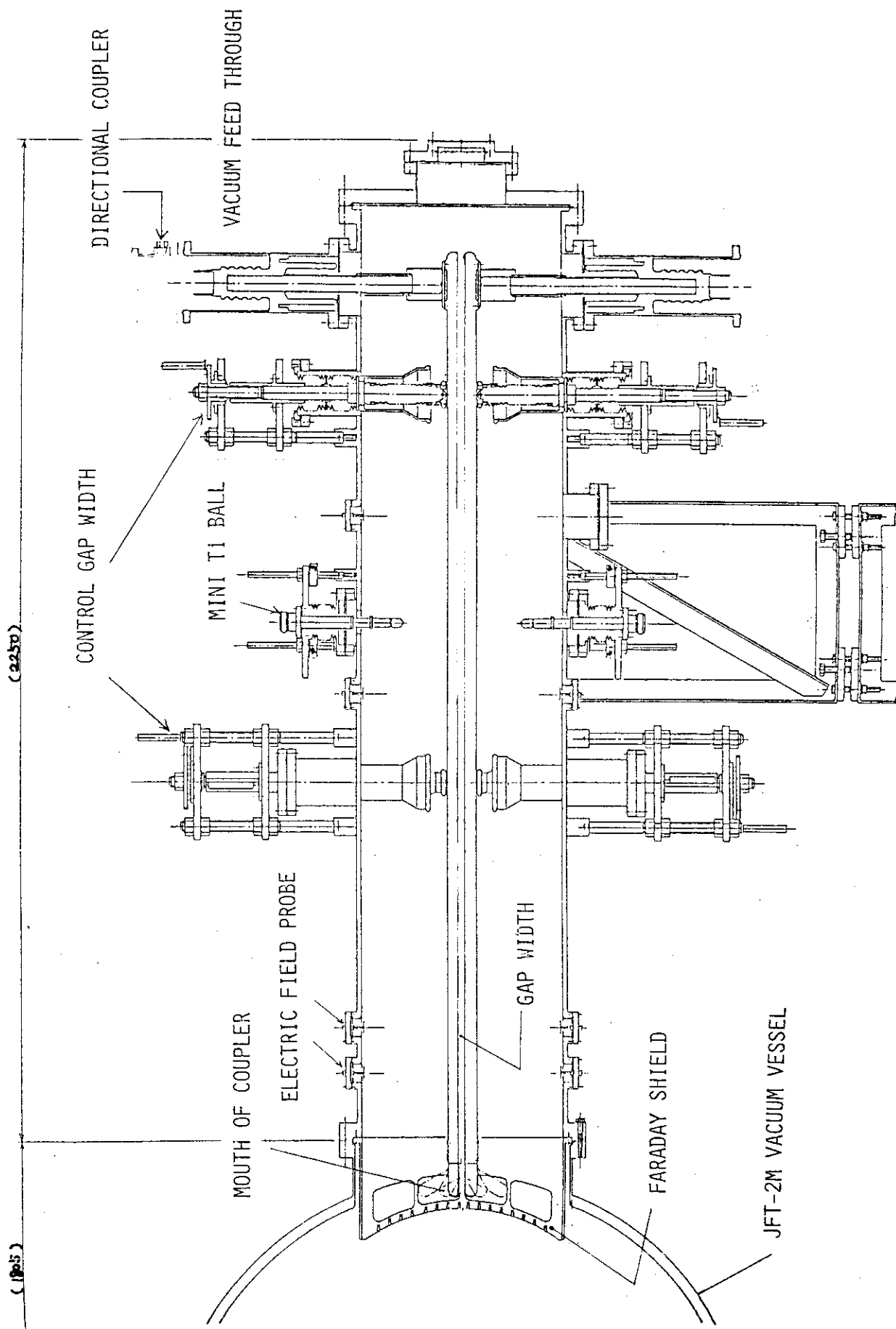


Fig.9 Figure of TEM electric field coupler.

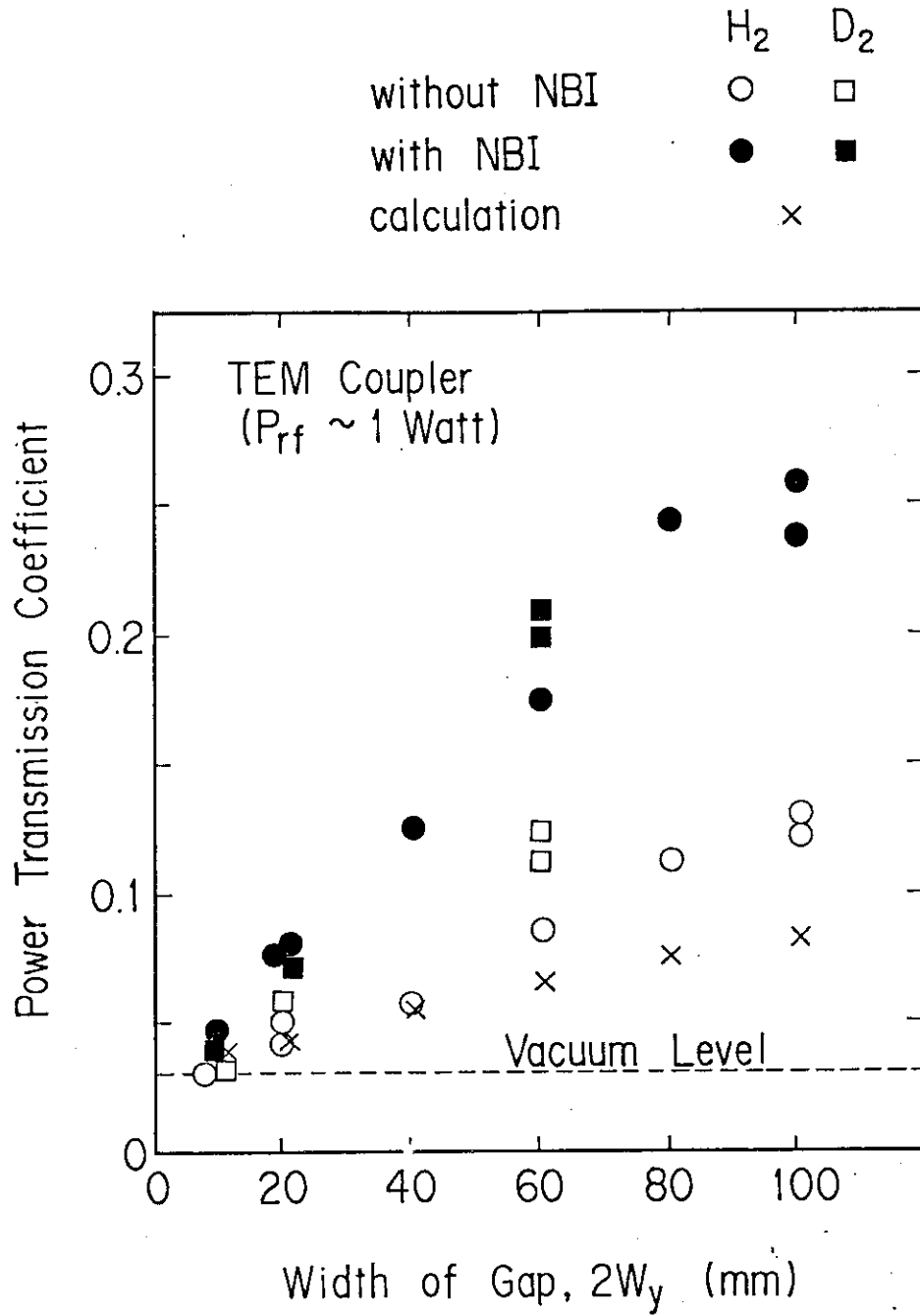


Fig.10 Transmission coefficient as a function of a gap distance between the two parallel plates.

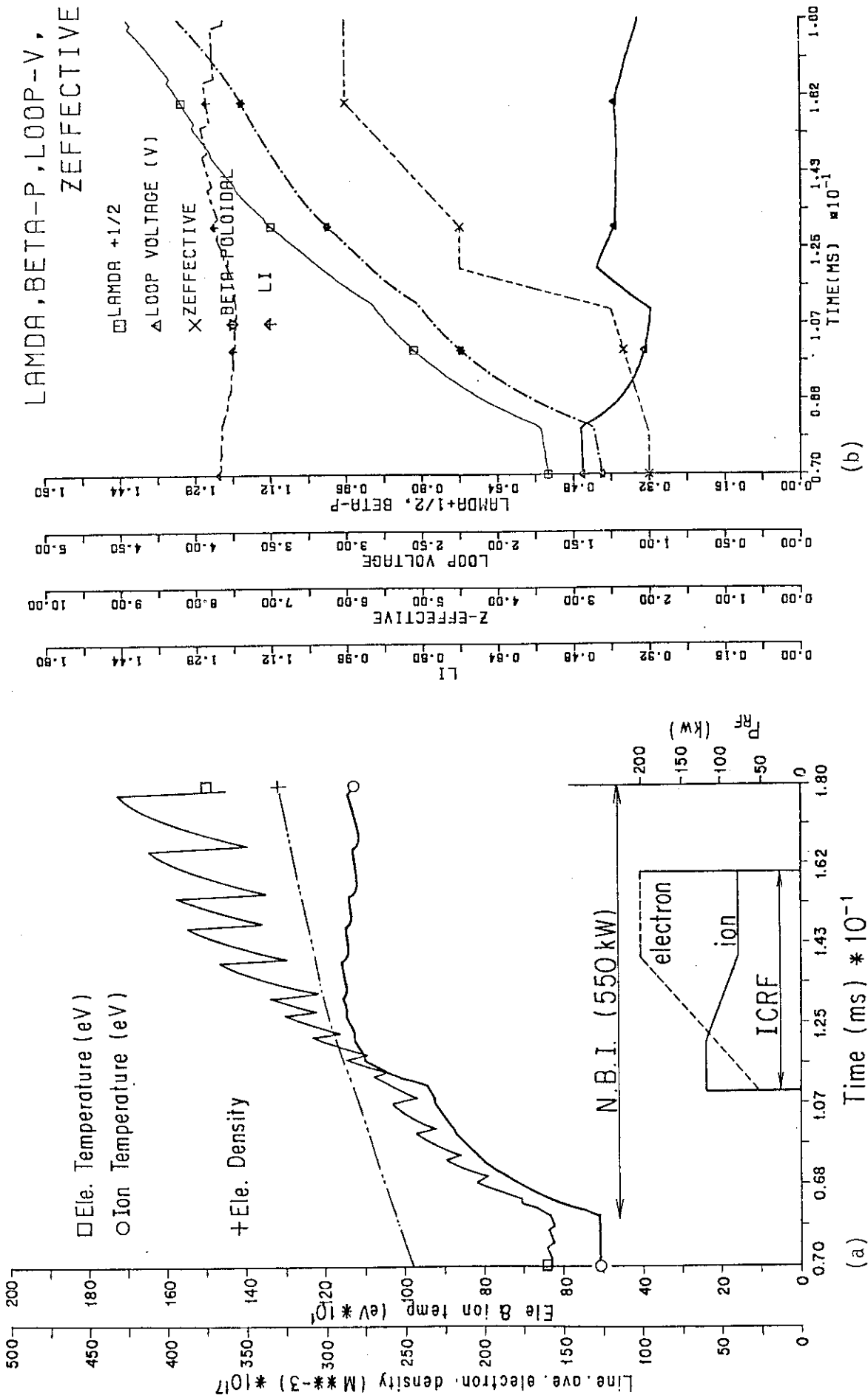


Fig.11 Results of the I-D tokamak code simulation. (a) Electron and ion temperatures. Also assumed time evolution of total RF deposition power on electrons and on ions are shown. (b) Assumed evolution of z-effective and the simulation results of $\Lambda+1/2$, loop voltage, β_p , and λ_i are shown.